7-2015

Development of a bi-national Great Lakes coastal wetland and land use map using three-season PALSAR and landsat imagery

Laura Bourgeau-Chavez
Michigan Technological University

Sarah L. Endres
Michigan Technological University

Michael Battaglia
Michigan Technological University

Mary Ellen Miller
Michigan Technological University

Elizabeth Banda
Michigan Technological University

See next page for additional authors

Recommended Citation

Bourgeau-Chavez, L., Endres, S. L., Battaglia, M., Miller, M. E., Banda, E., Laubach, Z., Higman, P., Chow-Fraser, P., & Marcaccio, J. (2015). Development of a bi-national Great Lakes coastal wetland and land use map using three-season PALSAR and landsat imagery. *Remote Sensing, 7*(7), 8655-8682.
http://dx.doi.org/10.3390/rs70708655
Retrieved from: https://digitalcommons.mtu.edu/mtri_p/13

Follow this and additional works at: https://digitalcommons.mtu.edu/mtri_p

 Part of the Ecology and Evolutionary Biology Commons, and the Environmental Sciences Commons

Remote Sens. **2015**, *7*, 8655-8682; doi:10.3390/rs70708655

OPEN ACCESS

remote sensing

ISSN 2072-4292

www.mdpi.com/journal/remotesensing

Article

Development of a Bi-National Great Lakes Coastal Wetland and Land Use Map Using Three-Season PALSAR and Landsat Imagery

Laura Bourgeau-Chavez [1,*], Sarah Endres [1,†], Michael Battaglia [1,†], Mary Ellen Miller [1,†], Elizabeth Banda [1,†], Zachary Laubach [1,†], Phyllis Higman [2], Pat Chow-Fraser [3] and James Marcaccio [3]

[1] Michigan Tech Research Institute, Michigan Technological University, Ann Arbor, MI 48105, USA; E-Mails: slendres@mtu.edu (S.E.); mjbattag@mtu.edu (M.B.); marymill@mtu.edu (M.E.M.); ecbanda@mtu.edu (E.B.); zchlaubach@gmail.com (Z.L.)

[2] Michigan State University Extension; Michigan Natural Features Inventory, Lansing, MI 48901, USA; E-Mail: higmanp@michigan.gov

[3] McMaster University, Hamilton, ON L8S 4K1, Canada; E-Mails: chowfras@mcmaster.ca (P.C.-F.); marcacjv@mcmaster.ca (J.M.)

† These authors contributed equally to this work.

* Author to whom correspondence should be addressed; E-Mail: lchavez@mtu.edu; Tel.: +1-734-913-6873; Fax: +1-734-913-6880.

Academic Editors: Alisa L. Gallant and Prasad S. Thenkabail

Received: 9 February 2015 / Accepted: 30 June 2015 / Published: 9 July 2015

Abstract: Methods using extensive field data and three-season Landsat TM and PALSAR imagery were developed to map wetland type and identify potential wetland stressors (*i.e.*, adjacent land use) for the United States and Canadian Laurentian coastal Great Lakes. The mapped area included the coastline to 10 km inland to capture the region hydrologically connected to the Great Lakes. Maps were developed in cooperation with the overarching Great Lakes Consortium plan to provide a comprehensive regional baseline map suitable for coastal wetland assessment and management by agencies at the local, tribal, state, and federal levels. The goal was to provide not only land use and land cover (LULC) baseline data at moderate spatial resolution (20–30 m), but a repeatable methodology to monitor change into the future. The prime focus was on mapping wetland ecosystem types, such as emergent wetland and forested wetland, as well as to delineate wetland monocultures (*Typha*,

Phragmites, *Schoenoplectus*) and differentiate peatlands (fens and bogs) from other wetland types. The overall accuracy for the coastal Great Lakes map of all five lake basins was 94%, with a range of 86% to 96% by individual lake basin (Huron, Ontario, Michigan, Erie and Superior).

Keywords: wetlands; synthetic aperture radar; PALSAR; Landsat; thermal; optical imagery; *Typha*; *Phragmites*; *Schoenoplectus*

1. Introduction

As the link between land and water, coastal wetlands of the Great Lakes serve major ecologic and economic roles contributing to the overall health and maintenance of the Great Lakes. These coastal wetlands provide habitat, sources of food, and breeding grounds for many common and regionally rare bird, mammal, herptile, and invertebrate species [1]. They also provide many other ecosystem services including water filtration, flood control, shoreline protection, and recreation. Managing such an important resource requires periodic mapping of the extent, type, and location of the wetlands and adjacent land use and land cover (LULC), as well as field monitoring of indicator variables such as water chemistry, water levels, and biodiversity of flora and fauna. Wetlands are highly vulnerable to both climatic [2] and anthropogenic changes such as drainage, dredging, filling, shoreline modification, water-level regulation, nutrient enrichment, introduction of non-native species, and road development. Historically, more than two-thirds of wetlands in the Great Lakes region have been drained for agriculture and other development [3], making the management of the remaining wetlands essential. Monitoring at a regional scale is necessary for effective coastal land and water management to understand and mitigate the increasing risk posed to the Great Lakes from LULC change and climatic influences.

The Great Lakes Coastal Wetland Consortium (GLCWC) developed a monitoring plan that is designed to not only assess the health and quality of the ecosystems, but also to provide a baseline for assessing effects of climate change and to provide key inputs to decision support for coastal management [4]. The monitoring plan requires a baseline map of wetland type and areal extent and adjacent land, as well as periodic updates. Such a map has been lacking in comprehensive form for the basin. In the past, mapping efforts have stopped at political boundaries. On the United States (U.S.) side there are the U.S. Fish and Wildlife Service's (USFWS) National Wetlands Inventory (NWI), National Oceanic and Atmospheric Administration's Coastal Change and Analysis Program (NOAA C-CAP), and a host of state-based maps such as the Ohio Wetland Inventory and Michigan's Integrated Forest Monitoring Assessment and Prescription. On the Canadian side, there are the Ontario Great Lakes Coastal Wetlands Atlas and the Canadian Wetland Inventory. To date, the best map of both the U.S. and Canada coastline has been the Great Lakes Coastal Wetland Inventory [5], which used a hydrogeomorphic classification scheme and integrated existing databases including the NWI, the Ohio Wetland Inventory, USFWS reports and hardcopy maps, and the Ontario Great Lakes Coastal Wetland Atlas. The Great Lakes Coastal Wetland Inventory includes the U.S. and Canada coastline and extends inland 1 km, but lacks information on

wetland stressors (e.g., LULC categories such as agriculture and urban) and is outdated (circa 1970s–80s). The mapping methods were mixed and the accuracy varied among the sources.

In 2010, under the Great Lakes Restoration Initiative, the U.S. Environmental Protection Agency (EPA) solicited the production of a map of the entire U.S. and Canadian coastal basin using a consistent methodology, such as the hybrid radar and optical satellite based approaches that had been demonstrated in a pilot study under the Great Lakes Coastal Wetlands Consortium [6]. That 2008 pilot study focused on archival Japanese Earth Resources Satellite 1 (JERS-1), Radarsat-1, and Landsat data and relied on existing maps and expert knowledge for training, rather than field data. The method included: (1) creating a categorical map from multi-date Landsat data; (2) creating a separate categorical map from multi-date JERS-1 and Radarsat-1 data; and (3) merging the two maps. A maximum likelihood classifier was used to create categorical maps for three 70 km × 70 km regions of the Great Lakes. The merged SAR-optical maps were found to have greater detectability of wetlands and reduced commission and omission errors, particularly for the wetland classes [6]. This pilot effort demonstrated the importance of using both optical and SAR data for mapping Great Lakes wetlands for three small areas of the Great Lakes and, thus, provided the basis for a complete mapping of the entire coastal basin. Since 2008, there have been many advances in remote sensing technology and software, as well as computing capability, which allow for such a large mapping effort with multiple datasets to be efficiently implemented.

The goal of the mapping effort presented in this article was to create a high accuracy map of not only wetlands, but also adjacent LULC for the Coastal Great Lakes basin such that the map could be used for management purposes to better understand the wetland distribution and wetland health through indicators of wetland stressors (*i.e.*, land use). The objective was to develop a mapping approach that utilized the fusion of moderate resolution (20–30 m) SAR and optical data from multiple seasons and integrated air photo interpretation and field data for training and validation to: (1) map broad land cover classes, with a focus on the wetland ecosystem classes (e.g., emergent, shrub wetland, forested wetland); (2) distinguish forested bog, open, shrubby and treed fen *versus* inundated shrub and forested wetlands (non-peat, swamps); (3) delineate monocultures of wetland plant species including invasive (*Typha spp*. and *Phragmites australis*) and non-invasive (*Schoenoplectus spp*.) species; and (4) target overall map accuracies greater than 90% and individual class accuracies greater than 70%. In this article, the approach and methods are detailed and the map results are presented and tested through accuracy assessments of independent datasets.

2. Background

Image fusion has long been used both to increase spatial resolution and classification accuracy by gaining additional spectral information [7]. Whereas several researchers have evaluated the use of optical or SAR data alone for mapping wetlands, until more recently few had evaluated SAR and optical fusion for wetland mapping [6,8–14] and most ignored the coarser-resolution thermal bands.

It has been well documented that multispectral data that include near-infrared (NIR) and shortwave infrared bands allow improved wetland detection and mapping over visible sensors alone because the near-infrared portion of the electromagnetic spectrum allows identification of plant and hydrologic wetland conditions [15]. Similarly, the thermal wavelengths, although often neglected in mapping efforts due to the coarse spatial resolution on satellite systems (e.g., Landsat 5 TM band 6 at 120-m resolution),

are of high utility for mapping wetlands. The fact that water has a high thermal inertia results in temperature differences between uplands and wetlands, thus allowing them to be distinguished. Despite these advantages of infrared and thermal data, optical sensors have limitations in dense vegetation settings, particularly for detection of inundation beneath a dense shrub or forest cover.

Synthetic Aperture Radar (SAR) data are capable of detecting flooding beneath a vegetation canopy, monitoring water levels and soil moisture, and distinguishing other biophysical vegetation characteristics such as biomass and structure. Several researchers have evaluated the utility of SAR for wetland mapping using single and multi-date single channel SAR data [16–18], and others have evaluated polarimetric SAR [19–23]. The horizontal send and horizontal receive (HH) polarization of SAR systems have long been known to improve distinction of swamp from other wetland classes and uplands [9,10,19,24,25] due to an enhanced double bounce effect from the water surface to the tree trunks and back to the sensor (or vice versa). Non-flooded forests have more diffuse scatter from the ground surface, and less energy is returned to the SAR sensor than for flooded forests. If the vegetation in a non-forested wetland is of great enough biomass relative to the L-band wavelength (~24 cm), then a strong return due to some double bounce scattering will occur in that case, as well, although the strength of the return is typically less than in a flooded forest. This allows for the detection of the large invasive *Phragmites australis* (*Phragmites*), for example, which tends to dominate large patches of wetlands with tall (up to 5 m), dense stems [26].

In addition to multi-sensor datasets, there are advantages to using multi-temporal imagery datasets, which capture differences in vegetation and flood condition over the course of a growing season [27,28]. A multi-temporal and multi-sensor image fusion approach was applied in the work presented here using Landsat 5 TM and PALSAR imagery. The impetus for using this combination was based on the need for the detection of the presence of surface water, both in open areas and beneath canopies, as well as for improved detection of vegetation type. Previous research has noted that in practice it is difficult to accurately classify wetland species types based solely on optical spectral characteristics [29,30]. However, fusion with a complementary sensor type, such as SAR, should allow for a larger set of wetland characteristics to be detected. Further, by using spring, summer, and fall imagery the phenological and hydrological characteristics that define different wetland types should be captured, allowing for improved mapping (Figures 1 and 2). As an example, much of the variation within the wetland landscape is confused when observing the region only at a particular time of year, such as in the summer Landsat 5 TM image of the St. Clair river delta (Figure 1 top center). However, when considering the phenological changes through the seasons (Figure 1 top row) better distinction of various wetland types in this river delta are revealed. The L-HH three-season false-color composite of this area (Figure 1 bottom center) shows variations in hydroperiod during spring, summer, and fall; and L-HV (horizontal send, vertical receive) composite shows variations in biomass in the different seasons (Figure 1 bottom right). The thermal channel of Landsat TM (band 6; Figure 1 bottom left and Figure 2) aids in distinguishing wetland (darker regions) from upland, but the specific wetland type classes are confused. The spectral signatures from Landsat 5 for the various wetland classes of the St. Clair River Delta show the importance of the NIR band (band 4) and the seasonal patterns of reflectance for the wetland types (Figure 2). The reflectance signatures are based on the mean of a minimum area of 500 ha for each class. For *Schoenoplectus*, band 4 reflectance is much lower than all other wetland types and it peaks in the fall (Figure 2) whereas all other wetland types peak in mid-summer. There is a similar trend for L-band

HV backscatter for *Schoenoplectus*, with a peak in the fall. *Typha*, on the other hand, peaks mid-summer in L-HV and L-HH backscatter, when most of the other wetland classes (except aquatic bed) are somewhat constant in backscatter between summer and fall. When using three seasons of data, each sensor appears to provide a unique set of information, which when used in combinations should provide a powerful means to distinguish different types of LULC, and in particular, different wetland types.

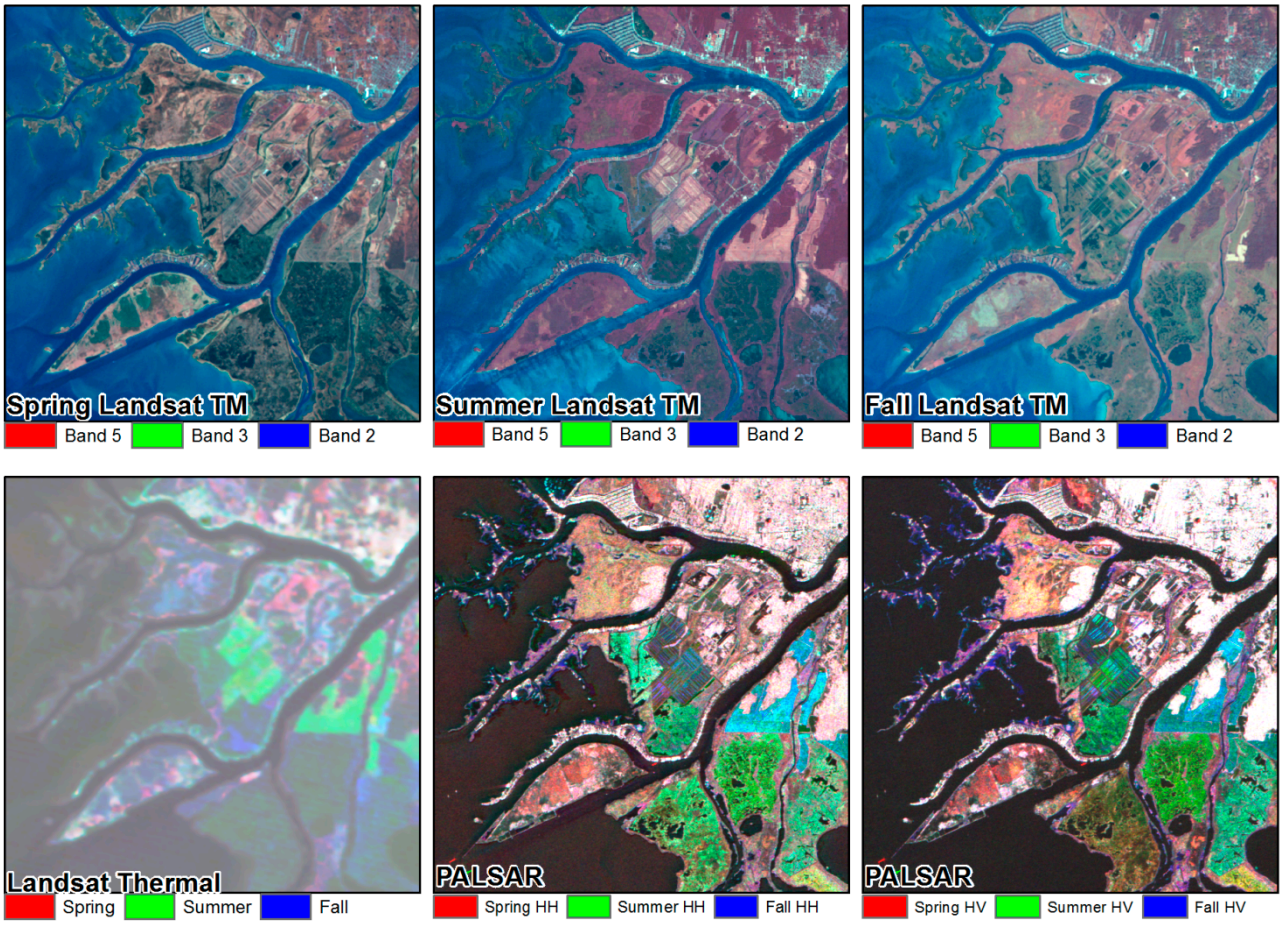

Figure 1. Multi-temporal and multi-sensor depiction of a large wetland complex on the St. Clair River Delta bordering the U.S. and Canada. Top row of images show spring, summer, and fall Landsat 5 TM imagery (bands 5, 3, 2). Bottom row shows Landsat 5 TM thermal false-color composite (spring, summer, and fall); PALSAR spring, summer, and fall HH false-color composite; and PALSAR spring, summer, and fall HV false-color composite. Image dates: Landsat spring = 5 May 2011, summer = 8 July 2011, fall = 9 October 2010; PALSAR spring = 26 May 2008, summer = 17 July 2010, fall = 17 October 2010.

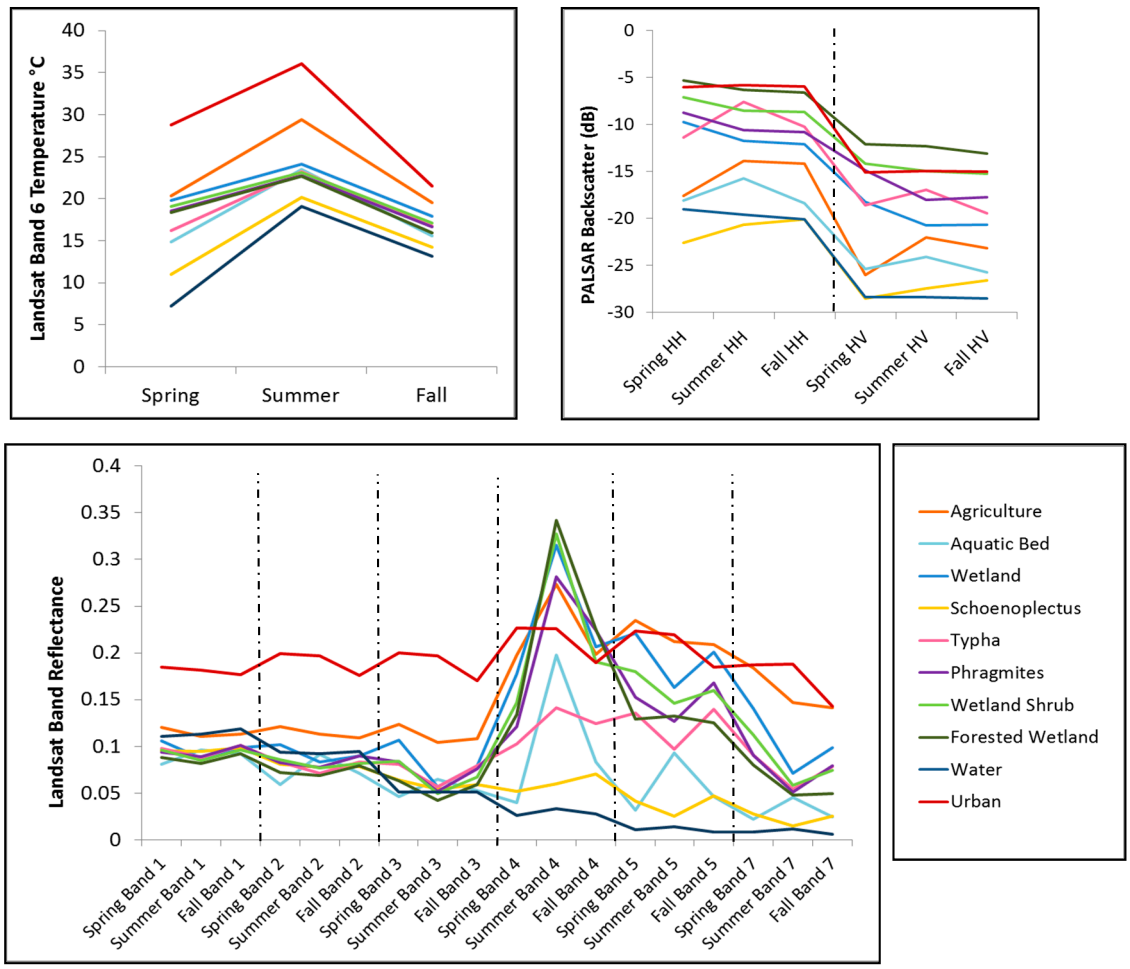

Figure 2. Plots showing spring, summer, and fall signatures for different land cover types: Landsat 5 TM band 6 temperature (top left), PALSAR L-band backscatter for HH and HV polarizations (top right), and Landsat 5 TM bands 1–5 and 7 for wetland classes and urban, water, and agriculture. Image dates are listed in Figure 1.

3. Methods

3.1. Study Area

The study area spans the United States and Canada coastline and the land within 10 km of the shoreline for lakes Ontario, Erie, Huron, Michigan, and Superior. In addition, included in the study area are the connecting waterways, consisting of Lake St. Clair and the St. Mary's, St. Lawrence, Detroit, and St. Clair rivers. The 10-km shoreline buffer provides coverage of coastal wetlands and additionally encompasses areas of hydrologic, biological, and geophysical transition between the interface of upland land cover and the deep-water boundary of the Great Lakes. Furthermore, a 10-km spatial extent captures the dynamics of anthropogenic influence, as land use interacts in a "downstream model" with surrounding land cover types. In total, the study area covers 9,056,410 ha inland in the U.S. and Canada, as well as captures all large offshore islands lying within the Great Lakes. Although the entire Great Lakes watershed affects the health of the coastal wetlands and the quality of water entering the lakes, mapping of areas further inland than the 10-km shoreline buffer was beyond the mapping goals and budget constraints.

3.2. Field Data

Field data on wetland ecosystem types were collected specifically for Great Lakes Restoration Initiative (GLRI) funded mapping projects and supplemented by other sources from independent projects throughout the 2007–2014 timeframe (Table 1). These supplemental datasets were systematically included or excluded, depending on their ability to assist image analysts. GPS locations had to have been collected within the wetland ecosystem for the field data to be usable, and the field data had to define an area that was at least the minimum mapping unit of the map to be produced (0.2 ha).

Table 1. Sources of field data collection used to aid in image interpretation. The top four sources were used for the development of training and validation data for the coastal Great Lakes map. The bottom two sources provided ancillary information.

Source	Region	Years of Collection	No. of Sites
MTU [1] (USGS [2]/USFWS funded)	USA: All 5 Lakes	2010–2011	1191
MTU (EPA funded)	USA and Canada: Lakes Huron, Superior, Erie, Michigan	2011–2014	147
McMaster University	Canada: Lakes Huron, Erie Ontario	2013	70
Michigan State University (EPA funded)	Canada: Lakes Superior, Huron, USA: Lake Michigan	2012–2013	343
Great Lakes Instrumentation Collaboratory (GLIC)	USA and Canada: All Lakes	2011–2013	--
McMaster University	Canada: Georgian Bay	2007–2009	249

[1] Michigan Technological University; [2] U.S. Geological Survey.

The main source of training and validation data came from extensive field campaigns in 2010–2011 under GLRI cooperative agreements with the USGS Great Lakes Science Center and USFWS for mapping areas of the problematic invasive species, *Phragmites*. That project was focused on mapping large stands of the invasive plant along the U.S. coastline; a detailed description of this methodology is outlined in Bourgeau-Chavez *et al.* [26]. From May–October in 2010 and 2011 field data were collected by regionally located teams at 1191 locations. Field-visited locations represented a pool of randomly selected data points primarily within the emergent wetland category of the NWI and additional observer-selected points of interest (see [26] for details). However, many of the field sites turned out to be forested or shrub wetlands. Field crews were instructed to supplement pre-selected random field points with additional opportunistic field points. The goal of additional observer-selected field points was to characterize and delineate areas of vegetative transition, possible unique spectral signals, and areas of likely classification confusion. At all field locations, data collections followed a standardized protocol. Field crews used a hand held GPS, a GPS camera, laminated maps of aerial photographs (30-cm to 1-m resolution), density grids, and tape measurers. At each location a vegetative index was constructed; wetland type was assigned, species diversity noted, dominant species composition assigned, water level measured, vegetation life stage recorded, and for *Phragmites* and *Typha spp.*, height and density measures were collected. Additionally, hand drawn maps and delineations of laminated aerial photograph maps distinguished unique vegetation types and species transition areas within wetland

complexes. Finally, geolocated photographs were taken in the four cardinal directions at a centralized location providing an additional layer of validation and ground truth for each data location. The *Phragmites* map product, as well as the data characterizing other LULC features, was used in the coastal wetland and upland mapping.

The field data collection methodology used as a part of the *Phragmites* mapping project provided the foundation on which subsequent field data collects were organized. During 2012–2014, the field campaign was extended to inform the basin-wide bi-national map on not only emergent wetland types, but also shrub, forest, and peatland classes, and to gather additional field data for the Canadian side of the basin. For this field effort, the locations of the field sampling were not random, but specifically selected to target those areas within the study region that were data-poor and/or for wetland classes that were unrepresented. An additional 560 field data locations were sampled in 2012–2014, with 70 locations provided by McMaster University with their 2013 collections along lakes Erie, Ontario, and Huron using the project field collection protocol. Additionally, McMaster had collected 249 field locations in 2007–2008 in Georgian Bay that provided ancillary information. Another source of field data was the vegetation species dominance metrics from the Fish and Invert database of the Great Lakes Instrumentation Collaboratory (GLIC) project, also funded by the GLRI. These data were not included in classification training or validation, but provided ancillary information to inform the image analysts for specific wetland classes. Upland areas were not field visited because the identification and delineation of upland classes were conducted using air photo interpretation techniques.

The wetland field data collection resulted in a total of 1751 sampled sites. All wetland field sites in the database were checked for quality by comparing the location and information input to the database against the original field sheet, site description, field photos, and GPS location from both the GPS camera and the Garmin GPS unit. The breakdown of field sites by dominant cover type (Figure 3) shows a fairly good distribution of field samples, however, there were some regions along northern lakes Superior and Huron that were inaccessible due to lack of roads and/or rough terrain. Only those field collections that were sampled with the project-designated sampling design, as described above, are shown on the map. There were additional locations (GLIC and 2007–2008 McMaster) used to aid the image interpreters in defining training polygons, as noted above.

3.3. Image Data

Satellite imagery from both Landsat 5 TM and PALSAR that were collected in three seasonal time frames (spring, summer, and fall) were used for the mapping. Most imagery was collected in 2010 for PALSAR, but additional years (2007–2011) were needed to fill gaps to obtain the triplicate datasets from the three seasons. Similarly, for Landsat 5 TM, due to cloud cover, multiple years of data were aggregated to obtain complete coverage of the entire coastline. Thus, the seasonal triplicates of Landsat 5 TM data spanned the time frame between the years of 2007 and 2011. Note that only spring data were available from PALSAR for 2011, as it went out of commission thereafter. Seasonal date cutoffs for imagery were based on an approximation of early growth after leaf flush (spring: April–May), peak growth (summer: June–August), and early senescence (fall: September–October). These dates were adjusted based on latitude within the basin; for example, spring was later in the northernmost reaches of the basin.

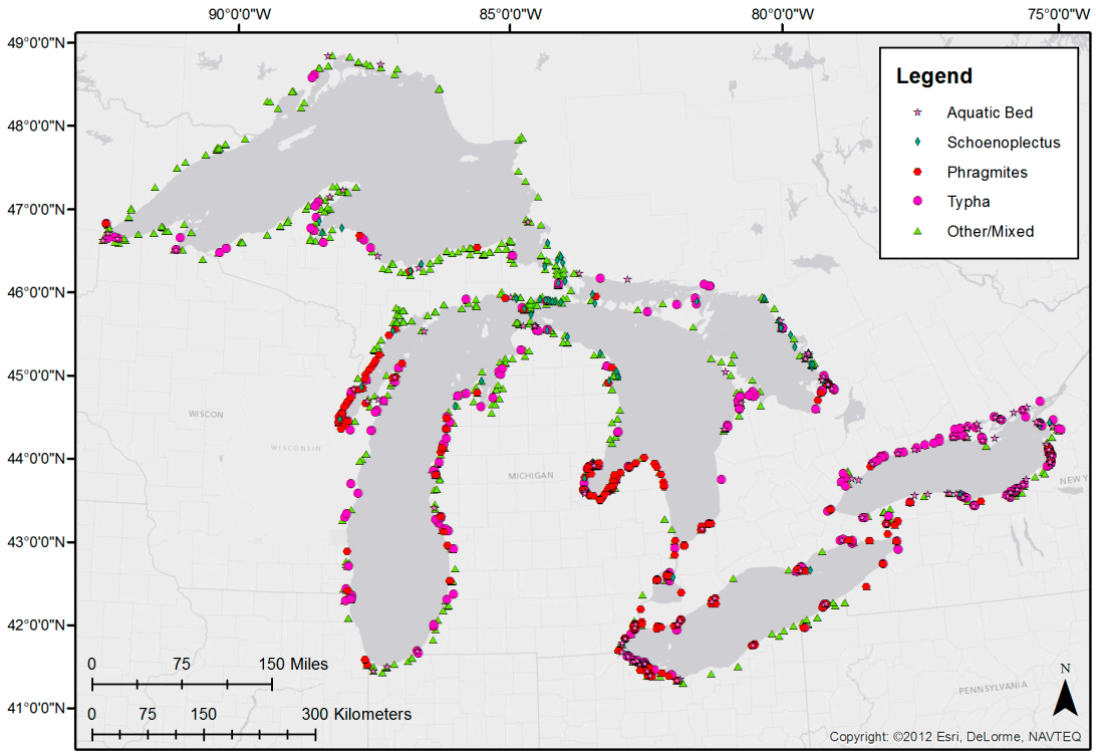

Figure 3. Map of field data locations, color-coded by dominant cover type. "Other/mixed" green triangles include all peatland, shrub, and forested wetland, as well as mixed emergent and wet-meadow wetlands.

Both Landsat 5 TM and SAR sensors required independent pre-processing procedures before the data were suitable for building a classified map. These steps are detailed in the sections below. After pre-processing, the images were combined into image stacks before being classified. The number of seasonal PALSAR scenes required to obtain the spatial and temporal coverage of the study area was 520 and the number of Landsat scenes needed was 159 (Table 2).

Table 2. Number of scene footprints required from each satellite sensor to map the coastal Great Lakes. Note that scenes covering Lake St. Clair are included in Huron.

Lake Basin	Number of PALSAR Scenes	Number of Landsat 5 TM Scenes
Erie	57	27
Huron	117	27
Michigan	107	26
Ontario	66	12
Superior	173	67

3.3.1. Landsat Data Selection and Processing

Image interpreters used EarthExplorer to identify and download clear Landsat 5 TM scenes acquired between the years of 2007–2011. When possible, the seasonal dataset for each area of interest (AOI; a PALSAR frame area) was created using scenes from the same year, and efforts were made to use the most recent imagery possible. For lakes Ontario, Erie, Huron, and Michigan the spring scenes were acquired in April and May, summer scenes were from June, July, August, and fall scenes were from

September and October. Lake Superior is farther north and green up typically occurs later, so the month of June was included in the spring scenes. Cloud-free imagery was not always available for the specified time frames; therefore, for some AOIs it was necessary to composite Landsat scenes from multiple dates. Julian day was included in each image stack to keep track of image sources. Multispectral Landsat TM data used in mapping coastal areas included bands 1–7 from spring, summer, and fall scenes. Optical bands were converted to radiance values, then to top-of-atmosphere (TOA) reflectance to normalize differences in illumination due to temporal changes in sun angle and earth-sun distance. The thermal bands were converted to TOA temperature brightness in degrees C assuming all pixels had an emissivity of water [31]. This assumption resulted in a relatively small underestimation of land surface temperature. Typically, in the warmer months the thermal difference between land and water is greater than the underestimation, making such an assumption suitable for mapping purposes.

Atmospheric correction using the latest Landsat Ecosystem Disturbance Adaptive Processing System (LEDAPS) software to convert Landsat digital counts to surface reflectance [32] is considered by many to be the best correction; however, we found TOA to produce comparable results with less computational burden. The effects of atmospheric correction were tested by comparing classification results using TOA reflectance and surface reflectance. Image classification and error analysis was then carried out using both TOA reflectance and LEDAPS surface reflectance. Atmospheric correction did not improve classification accuracy, but added considerable computational burden to each scene. Other previous large-scale mapping projects have found that using TOA reflectance values for image classification yielded more accurate results than using atmospherically corrected data [32–34].

Normalized Difference Vegetation Index (NDVI) images created from the visible-red (band 3) and NIR (band 4) bands [35] were also produced for inclusion in the map classification. This ratio works well for mapping green vegetation, as the reflectance in the red band is low due to absorption by chlorophyll and high in the near infrared band due to chlorophyll reflectance. The thermal and spectral indices allow for improved wetland detection and mapping over the optical sensors alone. All Landsat TM data and NDVI products were resampled using nearest neighbor to match the PALSAR Fine Beam Dual mode pixel size of 12.5 m and output as 32-bit data.

3.3.2. SAR Processing

SAR data for the study area were acquired from the Japanese ALOS PALSAR satellite, which has an L-band (~24 cm wavelength) SAR sensor. PALSAR data are collected in various modes, and for this project the single channel and dual channel modes were used. In Fine Beam Single mode (FBS), the sensor transmits and receives horizontally polarized signals (HH) with 10 m spatial resolution. In Fine Beam Dual mode (FBD), the sensor transmits horizontally polarized signals and receives horizontally and vertically polarized signals (HH and HV) with 20 m spatial resolution. PALSAR imagery used for this project was processed at the Alaska Satellite Facility (ASF) via a service contract. ASF downloaded the data from the ALOS satellite, processed, terrain corrected, and georeferenced it to within 1.5 PALSAR pixels (12.5 m), and delivered the 32-bit data with 12.5 m pixel spacing for the FBD data and 6.25 m pixel spacing for the FBS. Upon receipt, the FBS data were resampled using bilinear interpolation to match the FBD PALSAR pixel size of 12.5 m.

Once received from ASF, the data were checked to ensure geographic accuracy. Images that shared the same spatial extent were required to be within one pixel (12.5 m) of each other for mapping. If images did not meet this accuracy requirement they were processed through a co-registration algorithm. The SAR images were checked for alignment using Landsat TM images. If the SAR images were found to be misaligned they were georeferenced to a corresponding cloud-free Landsat 5 TM image. Spatial accuracy was calculated for each image using the root mean square error (RMSE). Lastly, a 3 × 3 median filter was applied to the PALSAR images to reduce speckle. Speckle is the coherent addition of backscatter from multiple scatterers in the same resolution cell. The result is random constructive and destructive interference, manifesting itself in bright and dark neighboring pixels, a "salt and pepper" effect. Because of speckle, a single pixel in SAR imagery cannot be used to measure features on the ground. Filtering of the data must be applied to reduce inherent speckle when producing a map.

3.4. Mapping Technique

Several image classification methods were evaluated, including hierarchical classification, object based image analysis (OBIA with eCognition), maximum likelihood (Erdas Imagine) classification of optical and SAR data separately and then recombination of the classes [6], and Random Forests (in R). Each of these approaches has advantages and disadvantages, and was evaluated for accuracy, consistency (between scenes and image analysts), and time consumption. These approaches were assessed in three experimental study areas with varying amounts of developed land (Northern Lake Michigan coastal wetland, Lake St. Clair coastal wetland, and Lake Huron coastal wetland). Random Forests [36] provided the best combination of high classification accuracy and time efficiency and was selected for our study. As a machine learning algorithm, Random Forests is an ensemble classifier consisting of multiple decision trees generated from a random subset of training data sites and bands from a stack of all data. Once the forest of decision trees is created, an individual pixel's classification is determined by which class receives the most "votes" across all decision trees. Random Forests is able to handle datasets with a small number of observations and a large number of attributes, is well suited to parallel processing, and is relatively insensitive to non-predictive inputs [37]. Additionally, the algorithm can easily handle missing attributes, such as cloud obscured pixels, as decision trees built without the missing attributes can be used to classify the compromised data.

A minimum mapping unit of 0.2 ha was used for the project. This unit was determined by application needs and limitations of the SAR imagery. Although the original multi-looked SAR imagery has 10–20 m resolution in the ground plane, due to inherent SAR image speckle the effective mapping unit must be a multiple of the resolution cell. Based on field data comparison with the fused Landsat-PALSAR map products and in reference to the coarsest SAR spatial resolution used (20 m), 0.2 ha, or 2 × 2.5 resolution cells, was the minimum size that could be confidently mapped [6].

The classification scheme applied to the datasets consisted of a combination of Anderson Level I upland classes [38], USFWS NWI classes, additional specific wetland classes (peatlands, invasive monotypic vegetation types including *Phragmites*, *Typha spp*., and *Schoenoplectus spp*.), and other upland classes that aided in improving map accuracy by reducing confusion (e.g., urban grass, fallow field). All upland and wetland classes are defined in Table 3.

The mapping process was iterative (Figure 4). First, wetland vegetation types were identified using field data and air photo interpretation. Next, polygons were drawn in ESRI ArcMap to spatially expand the field sampled locations and avoid edges of transitions between covertypes or land categories. These polygons were used as training and validation data, with a reserved priority of the field sampled sites for validation. Training data for uplands were created by image interpretation of current aerial photographs and were not field visited. Homeland Security Border 2009 Flight Imagery collected at 30-cm resolution was used for assessment of the coastlines of lakes Ontario, Erie, Huron, and Superior. The Border Flight data were not collected for Lake Michigan or Georgian Bay in Lake Huron, so a combination of publicly available satellite and aerial imagery was used. USDA National Agricultural Imagery Program (NAIP) 1-m data from 2009 to 2010 were used for Lake Michigan. For Georgian Bay, ESRI's World Imagery and Google Earth were used. These upland and wetland polygons provided the supervised training data and validation data (Figure 4). The supervised data were input to Random Forests with the three-date Landsat TM-PALSAR image stack that included all Landsat TM bands (21) and PALSAR bands (6), as well as an NDVI layer for each Landsat TM date (3), for a total of 30 input remote sensing bands. Post-classification, the classified images were filtered to eliminate isolated pixels and reduce the errors introduced by mixed pixels. Each classified pixel's value was replaced by the majority class of its eight neighbors using the ESRI majority filter. This resulted in the reduction of some errors at the expense of some correctly classified small linear features.

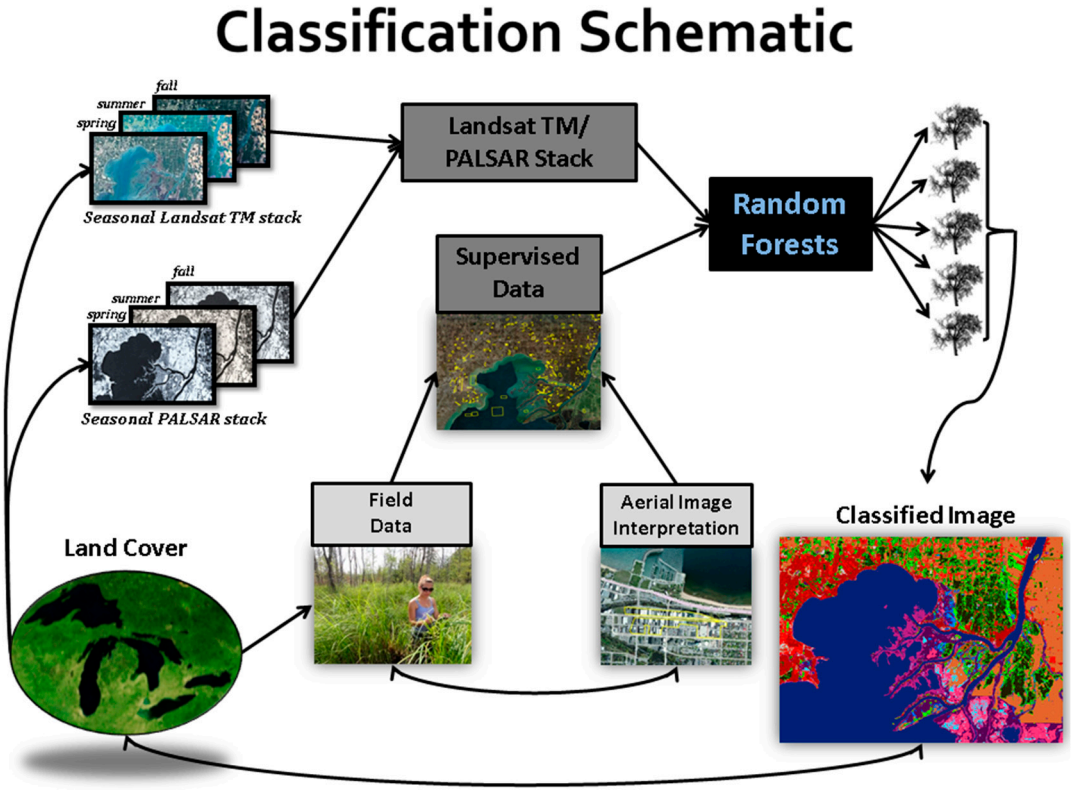

Figure 4. Schematic showing the mapping methodology from field data, aerial image interpretation, and satellite imagery to classified map.

Table 3. Description of each class mapped.

Class	Description
Urban	Residential areas, cites, towns, industrial areas, utilities, commercial services where the manmade structures have >75% coverage.
Suburban	Primarily residential areas where manmade structures (*i.e.*, buildings, farm equipment) are present, with more than or equal to 25% vegetation (trees, shrubs, grass) interspersed.
Urban Grass	Lawns, golf courses, athletic fields, urban parks, and mowed transitional zones such as medians or airfields.
Urban Road	Linear transportation routes, large driveways, and parking areas. Transportation routes can include highways, small two-lane roads, railroad beds, airfield landing areas, parking lots, and off- and on-ramps.
Agriculture	Hay fields and croplands where row crops such as corn, beans, and grains are in production. Land used for production of food or fiber; land use distinguishes agricultural land from similar natural ecosystem types (*i.e.*, wetlands and rice paddies).
Fallow Field	Agriculture fields not in row crop production, such as areas of native grasses or meadows and pastures.
Orchard	Orchards, vineyards, and ornamental plants/trees.
Forest	Broadleaf and needle leaf deciduous and evergreen trees and dead forests. Characterized by woody vegetation with a height >6 m. Crown closure percentage (*i.e.*, aerial view) >75%.
Pine Plantation	Needle leaved deciduous and evergreen trees with distinct row structure and typically planted in defined geometric plot. Crown closure percentage (*i.e.*, aerial view) >75%.
Shrub	True shrubs, immature trees, or stunted growth trees/shrubs. Characterized by woody vegetation with a height <6 m. May represent a successional growth stage that has not yet matured to forest, or stable communities of shrubs and stunted growth trees. Crown closure percentage (*i.e.*, aerial view) >50%.
Barren Light	Salt flats, beaches, sandy areas, bare rock, strip mines, quarries, gravel pits, and transitional areas (on gray scale >50% white). Land with limited ability to support life. Contains less than 33% vegetative cover. May include thinly dispersed scrubby vegetation.
Barren Dark	Salt flats, beaches, sandy areas, bare rock, strip mines, quarries, gravel pits, and transitional areas (on gray scale ≥50% black). Land with limited ability to support life. Contains less than 33% vegetative cover. May include thinly dispersed scrubby vegetation.
Water	Streams, canals, rivers, lakes, estuaries, reservoirs, impoundments, and bays. Areas persistently inundated by water that do not typically show annual drying out or vegetation growth at or above the water's surface. Depth of water column is >2 m, such that light attenuation increases significantly and surface and subsurface aquatic vegetation persistence declines or is less detectable.

Table 3. *Cont.*

Class	Description
Aquatic Bed	Algal beds, aquatic mosses, rooted vascular plants (e.g., eelgrasses and sea grasses, pond weeds, lily pads, milfoil) and floating vascular plants (e.g., lemna, water hyacinth, coontails, and bladderwarts). Inundated wetlands or water <2 m (excluding deep water zones). Habitats dominated by plants that grow principally on or just below the water's surface.
Wetland	Emergent wetland and wet meadow vegetation not represented by other classes. These are areas where the water table is at or near the Earth's surface. Seasonal inundation and/or drying are common. Vegetative species distributions are strong indicators of wetland condition. Does not include cultivated wetlands, such as rice paddies or cranberry farms.
Schoenoplectus	Dominate species is *Schoenoplectus spp.* and crown closure percentage (*i.e.*, aerial view) >50%.
Typha	Dominate species is *Typha spp*. and crown closure percentage (*i.e.*, aerial view) >50%.
Phragmites	Dominate species is *Phragmites australis* and crown closure percentage (*i.e.*, aerial view) >50%.
Open Peatland	Brown and graminoid moss dominated with >30 cm peat. Connected ground and surface water flow; minerotrophic. Crown closure percentage (*i.e.*, aerial view) >75%.
Shrub Peatland	Brown and graminoid moss dominated with >30 cm peat. Connected ground and surface water flow; minerotrophic. May represent a successional stage growth that has not yet matured to forest, or stable communities of shrubs and stunted growth trees. Crown closure percentage (*i.e.*, aerial view) >50%.
Treed Peatland	Brown and graminoid moss dominated with >30 cm peat. Connected ground and surface water flow; minerotrophic. Characterized by woody vegetation with a height >2 m. May represent a successional growth stage that has not yet matured to forest, or stable communities of shrubs and stunted growth trees. Crown closure percentage (*i.e.*, aerial view) >75%.
Wetland Shrub	Wetlands dominated by shrubs <6 m in height. Crown closure percentage (*i.e.*, aerial view) >50%.
Forested Wetland	Wetlands dominated by woody vegetation (dead or alive) >6 m in height. Includes seasonally flooded forests. Crown closure percentage (*i.e.*, aerial view) >50%.

The mapping process (Figure 4) was applied individually to AOIs nominally defined by each 70 km × 70 km PALSAR frame area (Figure 5). This approach was required because even small differences in adjacent PALSAR scene collection dates can result in great differences in SAR backscatter, depending on moisture conditions. The study area also covered a transition in ecoregions from southern boreal in the north to temperate conditions in the south, and a range in LULC from primarily rural in the north to highly urban in the south. An effort was made to collect field data within each 70 km × 70 km frame area for training. Note that there were small areas of the map that did not have PALSAR imagery available. These were generally slivers of the map where overlapping PALSAR coverage was unavailable for the seasons used in mapping. In these cases the maps were produced solely from Landsat 5 TM data. Once all of the AOIs were completely mapped, they were mosaicked to the extent of each of the five lake basins and accuracy was assessed.

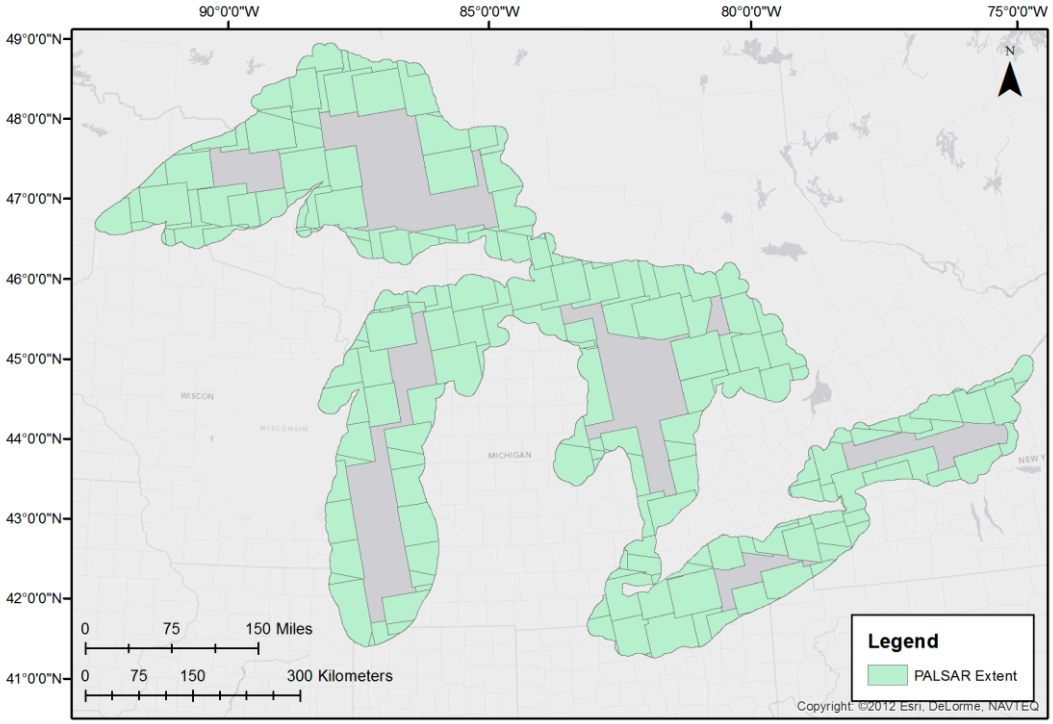

Figure 5. Map of extent of each area of interest (AOI) mapped. The AOIs are based on PALSAR image extents within the 10 km coastline buffer. Due to overlap of scenes, some AOIs are smaller than the full 70 km × 70 km PALSAR extent.

3.5. Accuracy Assessment

To ensure a robust set of validation data (polygons) for the Great Lakes coastal wetland maps, a percentage of the input training polygons was reserved for validation. Specifically, this was carried out by setting aside 20% of the training polygons as validation for each class. Whole polygons, not partial polygons, were set aside. The validation data were prioritized to include polygons derived from field verified sites. If less than 20% of a class's training polygons included field sites, then polygons derived from photo interpretation were also reserved. When more than 20% of the polygons were field verified, then validation polygons were randomly selected to be included in the training data. The average number

of validation polygons per class was 328, exceeding the 75–100 recommended by Congalton and Green 2008 for large areas [39].

The Random Forests algorithm generates an "out of bag" estimate of classification accuracy using the random subset of training data not used in generating each tree. However, these data are used to generate other trees within Random Forests and, thus, they are not independent. The "out of bag" accuracy was typically inflated compared to the independent assessment. Therefore, to ensure a robust and independent validation set, all accuracies presented in this article are based on the twenty percent of the training data that were reserved for validation.

4. Results

The mapping was completed in the summer of 2014 for all five lake basins (Figure 6). The results are presented below for the whole Great Lakes Basin and can be viewed on a webpage and requested for download [40]. The area of wetland mapped by class type in each lake basin is shown in Table 4. A total of 2,200,631 ha of wetlands were mapped in the bi-national Great Lakes coastal region to within 10 km of the coastline. This represents 24% of the total land area within the study extent (9,056,410 ha mapped). Of these coastal wetlands, a majority were forested or shrubby wetlands (18.2% of mapped area), with 3.7% of the mapped area representing emergent wetland types. Within the emergent wetland class, 24% of the area mapped was dominated by *Typha spp*. and 11% was dominated by invasive *Phragmites*.

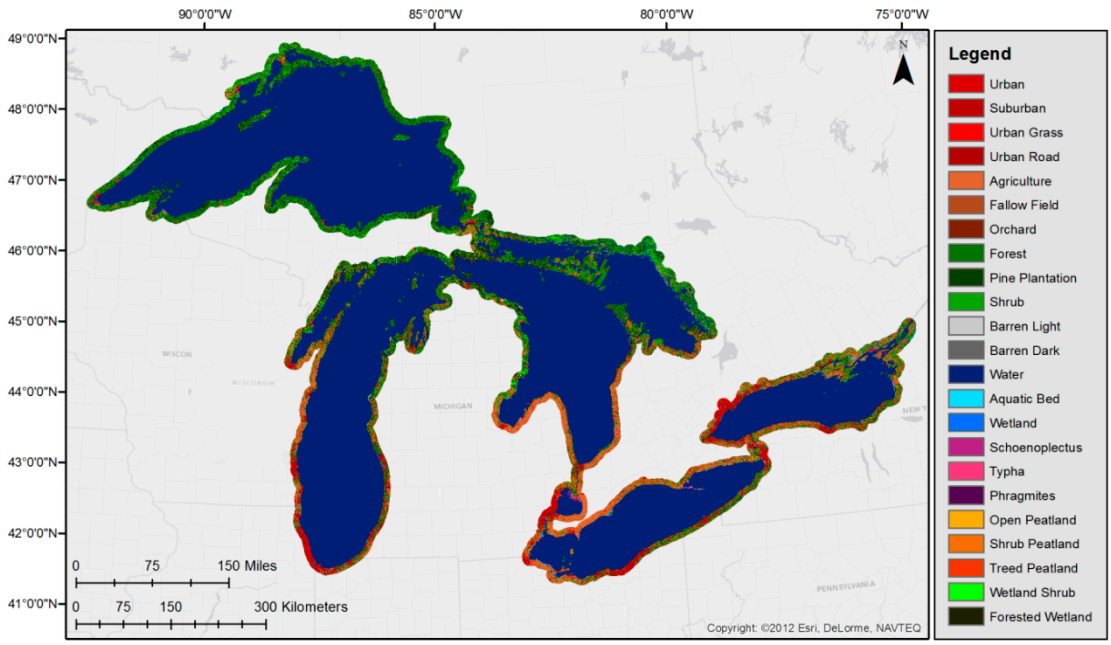

Figure 6. LULC map of the coastal Great Lakes, with a total accuracy of 94%.

The targeted goal for overall accuracy was 90% and the goal for individual classes was 70% accuracy. The overall accuracy of the entire basin map is 94% (Table 5), and for individual lakes it is greater than 90% for all lakes except Ontario, which is 86% (Table 6). If water is excluded, then overall accuracy reduces to 85%–87% and when all the wetland classes are lumped, overall wetland class accuracy is 75%–82%.

Table 4. Summary of area mapped by wetland class type (ha) and percentage of each class type mapped within the study area.

Wetland Type	Lakes Erie and St. Clair	Lake Ontario	Lake Michigan	Lake Huron	Lake Superior
Emergent (including *Typha* and *Phragmites*)	63,216	53,800	54,921	97,201	63,166
Typha	18,707	19,552	15,190	18,906	6509
Phragmites	20,129	2036	8851	6266	0
Woody Wetlands (Ha: Shrub and Forest)	111,049	108,738	361,307	525,446	539,624
Peatland (Bogs and Fens—open and woody)	0	0	11,522	33,439	46,635
Total Wetlands	194,527	179,570	447,005	708,647	670,882
Total Mapped Area	1,280,800	1,224,930	1,746,030	2,508,840	2,295,810
% Area Mapped as Wetland	15.2%	14.7%	25.6%	28.2%	29.2%
% Area Mapped as Emergent Wetland	4.9%	4.4%	3.1%	3.9%	2.8%
% Area Mapped as Woody Wetland	8.7%	8.9%	20.7%	20.9%	23.5%

The producer's accuracy represents how well the reference pixels are classified, whereas the user's accuracy represents the probability that a classified pixel actually represents that class on the ground. For individual classes for the entire basin, all of the producer's class accuracies are greater than 69% and all of the user's accuracies are greater than 61% except for one class, *Schoenoplectus* (35%; Table 5).

A single AOI covering the St. Clair Flats area provides an example of the details of the map (Figure 7). The St. Clair Flats is home to a large river delta wetland complex with a variety of herbaceous and woody wetlands, including large expanses of the invasive *Phragmites* and *Typha spp*., as well as large areas of *Schoenoplectus spp*. along the coastline. For this AOI, most of the producer's class accuracies are greater than 70%, except wetland, which is 65%, and all of the user's accuracies are greater than 70%, except wetland (38%), *Schoenoplectus* (59%), and forested wetland (60%; Table 7).

One of the outputs of Random Forests is a plot of band importance (mean decrease in accuracy). The mean decrease in accuracy is computed by permuting the out-of-bag data [38]. For each tree, the prediction error on the out-of-bag portion of the data is recorded and then the calculation is repeated after permuting each predictor (input band) variable. The difference between the two are then averaged over all the trees, and normalized by the standard deviation of the differences. The band importance from the mean decrease in accuracy plot for the St. Clair Flats AOI, which is dominated by wetlands (Figure 8), was very different than the plot for all 40 AOIs over Lake Michigan, of which a majority of the landscape was upland classes (Figure 9). For the wetland dominated AOI (Figure 8), the three most important bands were spring Landsat TM NDVI, spring Landsat TM thermal, and spring L-HH, followed by L-HV from summer and L-HH from fall. In contrast, for the upland dominated landscape (Figure 9) the three most important bands were the Landsat TM thermal (band 6) from spring, NIR (band 4) from spring, and NIR from fall. PALSAR L-HV from spring was 12th in band importance, with the other two HV bands at 14th and 15th, and the HH bands at 17–19th in importance.

Table 5. Error matrix for all coastal Great Lakes. Numbers represent pixels. Some classes have been collapsed to higher-order classes for display purposes.

Classified	Ground Truthed Values																
	Urban	**Agriculture**	**Forest**	**Shrub**	**Barren**	**Water**	**Aquatic Bed**	**Wetland**	***Schoeno-plectus***	***Typha***	***Phragmites***	**Peatland**	**Shrub Wetland**	**Forested Wetland**	**Sum**	**Comm-ission**	**User Acc.**
Urban	55,555	7257	315	519	4222	204	26	31	0	139	64	11	94	9	68,446	19%	81%
Agriculture	1575	650,640	452	3051	1149	65	82	585	0	121	61	13	394	43	658,231	1%	99%
Forest	88	1714	108,758	3027	39	15	14	145	3	12	14	173	1174	5069	120,245	10%	90%
Shrub	381	5625	3034	123,911	290	44	32	470	8	78	34	351	2775	3097	140,130	12%	88%
Barren	534	1979	7	80	43,168	566	0	38	0	63	1	0	24	0	46,460	7%	93%
Water	0	0	0	20	363	184,5154	324	1	96	7	0	15	4	8	1,845,992	0%	100%
Aquatic Bed	40	1034	0	31	64	7597	17,777	534	233	144	103	92	153	157	27,959	36%	64%
Wetland	165	3232	37	372	83	70	362	13,083	99	848	226	319	2359	92	21,347	39%	61%
Schoenoplectus	2	2	0	2	1313	2065	375	290	2256	52	12	32	22	0	6423	65%	35%
Typha	15	1514	16	175	38	43	423	1143	22	17,631	333	44	207	70	21,674	19%	81%
Phragmites	52	2360	47	26	10	114	99	667	1	694	7775	0	210	77	12,132	36%	64%
Peatland	19	427	236	878	28	13	45	168	1	83	0	14,945	1475	165	18,483	19%	81%
Shrub Wetland	209	1676	1595	3454	33	7	105	1432	8	250	84	828	27,942	3910	41,533	33%	67%
Forested Wetland	30	183	4261	4523	8	42	36	52	2	13	1	353	3804	63,097	76,405	17%	83%
Sum	58,665	67,7643	118,758	140,069	50,808	1,855,999	19,700	18,639	2729	20,135	8708	17,176	40,637	75,794			
Omission	5%	4%	9%	13%	15%	1%	10%	30%	17%	14%	11%	13%	31%	17%			
Prod. Acc.	95%	96%	92%	88%	85%	99%	90%	70%	83%	88%	89%	87%	69%	83%			94%

Table 6. Summary of classification accuracy by lake basin. Included is the accuracy for wetland classes with water removed.

Lake Basin	Overall Accuracy	All Classes Except Water	Wetlands Classes Only
Erie	**92%**	85%	82%
Ontario	**86%**	85%	81%
Huron	**93%**	85%	75%
Michigan	**96%**	87%	82%
Superior	**95%**	86%	82%

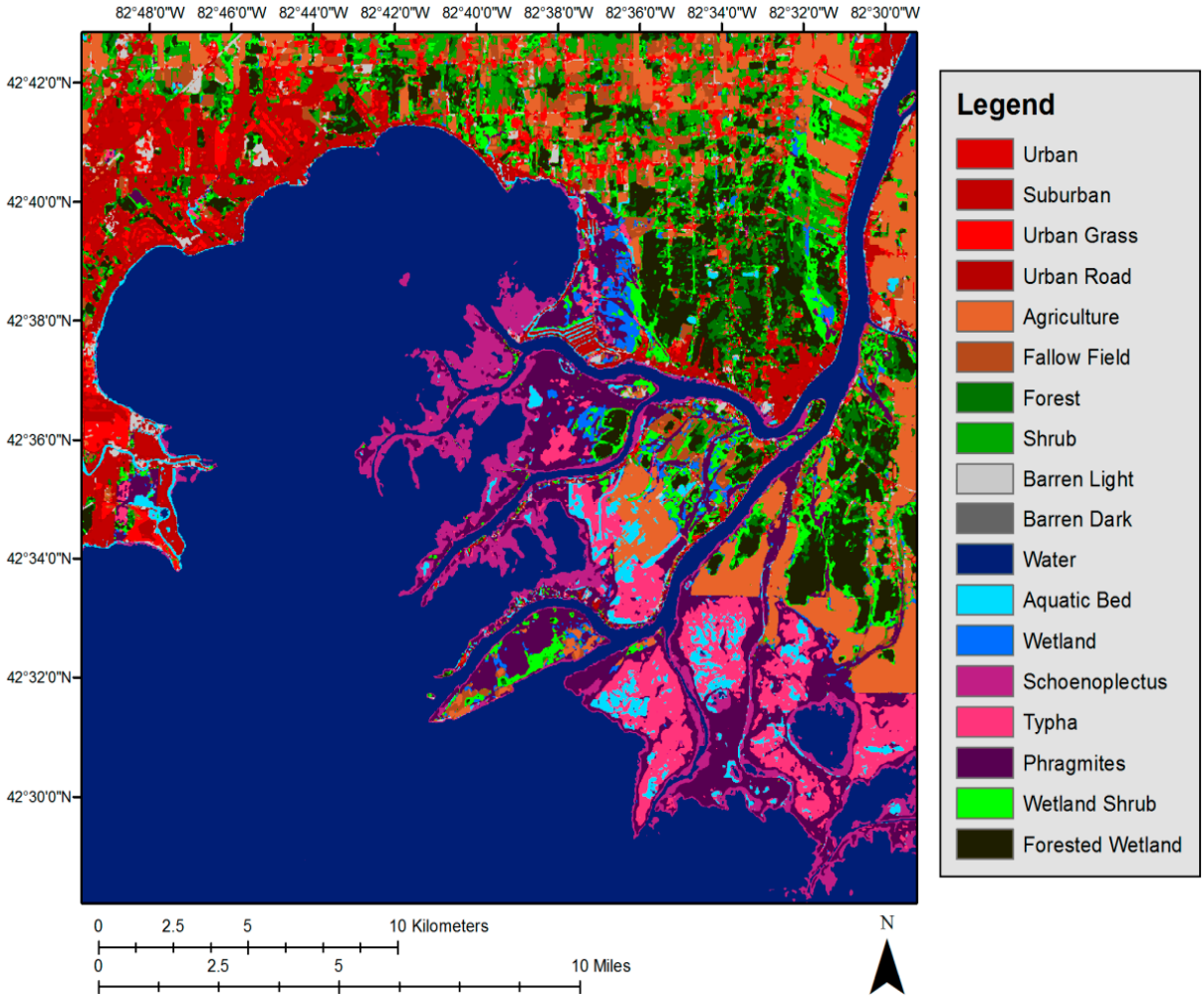

Figure 7. Map of wetland type and LULC for the St. Clair Flats AOI. Overall accuracy is 97.5%.

Table 7. Error Matrix for the St.Clair Flats AOI. Numbers represent pixels. Some classes have been collapsed into higher-order classes for display purposes.

Classified	Ground Truthed Values															
	Urban	**Agriculture**	**Forest**	**Shrub**	**Barren**	**Water**	**Aquatic Bed**	**Wetland**	***Schoeno-plectus***	***Typha***	***Phragmites***	**Shrub Wetland**	**Forested Wetland**	**Sum**	**Comm-ission**	**User Acc.**
Urban	1744	46	0	0	175	0	0	0	0	0	8	0	0	1973	12%	88%
Agriculture	5	30,197	5	147	0	0	2	19	0	0	13	43	0	30,431	1%	99%
Forest	0	1	214	11	0	0	0	0	0	0	0	52	0	278	23%	77%
Shrub	0	44	0	2700	0	0	0	4	0	0	0	153	0	2901	7%	93%
Barren	123	89	0	0	860	0	0	0	0	0	0	0	0	1072	20%	80%
Water	0	0	0	0	0	80,981	0	0	5	2	0	0	0	80,988	0%	100%
Aquatic Bed	0	0	0	0	0	15	347	0	0	0	0	0	0	362	4%	96%
Wetland	0	56	0	0	0	0	0	53	0	0	23	9	0	141	62%	38%
Schoenoplectus	0	0	0	0	0	166	1	0	283	27	0	0	0	477	41%	59%
Typha	0	2	0	0	0	0	25	0	0	1000	0	1	0	1028	3%	97%
Phragmites	0	76	0	0	0	4	17	5	0	100	1170	13	0	1385	16%	84%
Shrub Wetland	0	0	0	17	0	0	0	0	0	1	32	733	0	783	6%	94%
Forested Wetland	0	2	45	0	0	0	1	0	0	0	0	22	106	176	40%	60%
Sum	1872	30,513	264	2875	1035	81,166	393	81	288	1130	1246	1026	106			
Omission	7%	1%	19%	6%	17%	0%	12%	35%	2%	12%	6%	29%	0%			
Prod. Acc.	93%	99%	81%	94%	83%	100%	88%	65%	98%	88%	94%	71%	100%		97.5%	

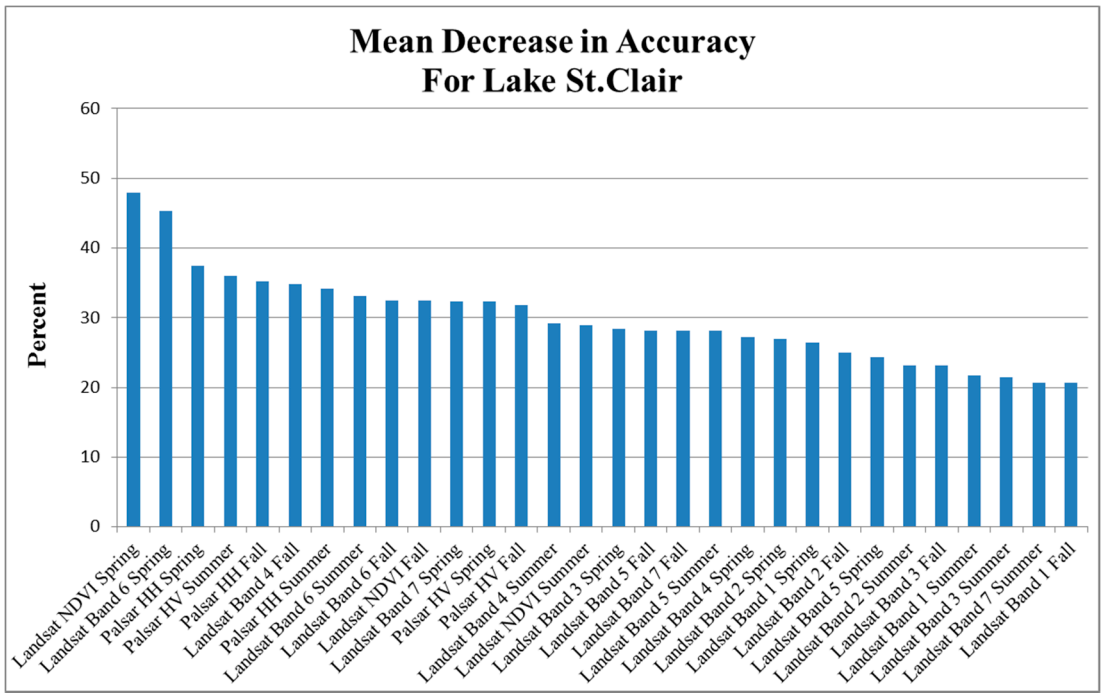

Figure 8. Band importance for the wetland dominated Lake St. Clair Flats computed from Random Forests.

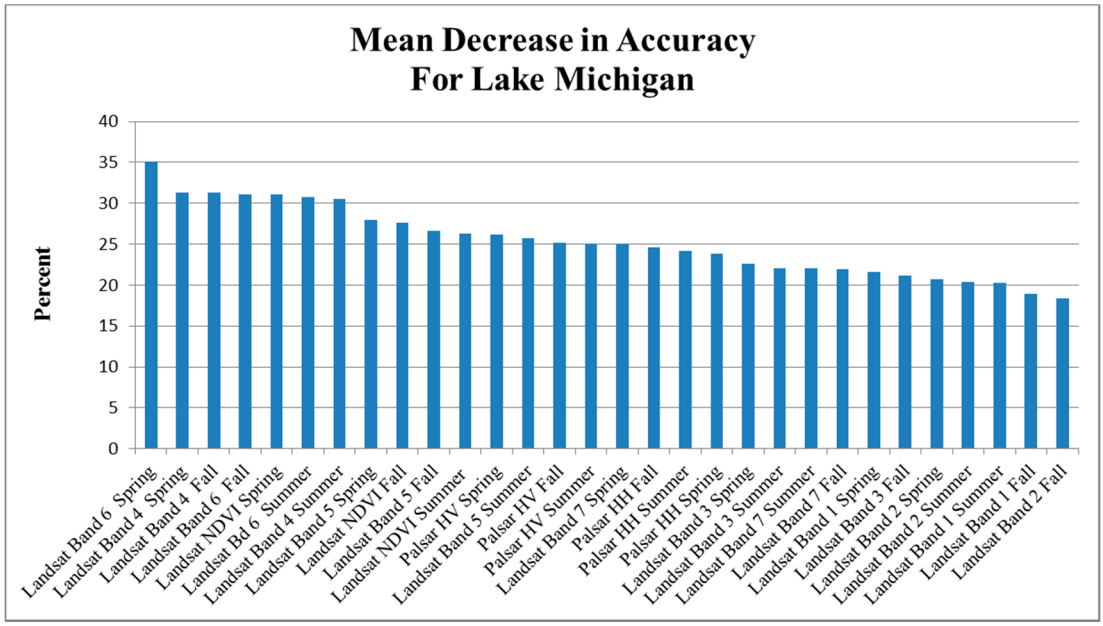

Figure 9. Average band importance for 40 AOIs in the upland dominated Lake Michigan Basin computed from Random Forests.

5. Discussion

5.1. Accuracy and Confusion Classes

The overall accuracy for the coastal Great Lakes maps was 94%, with a range from 86% to 96% overall accuracy by lake basin (Huron, Ontario, Michigan, Erie, Superior). This overall accuracy is slightly higher than the rates of 80%–89% achieved in other large-area mapping projects around the

world [14,28,31,41,42] and comparable with the rate of 95% achieved for Alaska [16]. For the coastal Great Lakes maps, a few wetland classes had individual accuracies below the targeted 70% producer's and user's accuracies. For example, *Schoenoplectus spp.* had a producer's accuracy of 83% and a user's accuracy of only 35% for all the Great Lakes (Table 5). The low user's accuracy suggests only 35% of all *Schoenoplectus spp.* pixels are indeed *Schoenoplectus spp.* on the ground. *Schoenoplectus spp.* proved difficult to map because the plants often grow in narrow, patchy stands along the coast. *Schoenoplectus* stands are also much less prevalent than the more common large monotypic stands of *Typha spp.* or *Phragmites. Schoenoplectus spp.* are often seen mixed with other vegetation and patches of open water or floating aquatics which can explain the confusion with the generic wetland class, aquatic bed, and open water classes. In areas dominated by wetlands, such as the St. Clair Flats AOI, the accuracy of *Schoenoplectus spp.* improves, with a producer's accuracy of 98% and a user's accuracy of 59% (Table 7). The specific dominant cover wetland classes could be collapsed into a higher-order class (e.g., *Typha* and *Phragmites* could be collapsed into "wetland" (NWI emergent wetland class; see Tables 4 and 6) to increase the map accuracy. However, in many cases the major confusion is with similar or higher-order wetland classes, and lower accuracy of a specific cover type is compensated by the general ability to distinguish differences among classes. *Schoenoplectus* may be better collapsed with open water in many regions. For this genus a shorter wavelength SAR, such as C-band (~5.7 cm), would likely improve mapping.

In some regions of the map, specifically those areas that are more developed, accuracies are slightly lower because of the higher variability in LULC over small spatial extents. In these areas, there are some noticeable classification discrepancies because of mixed pixel effects. For example, an area that transitions from urban to emergent wetland may show false instances of other classes in pixels where the transition occurs. Another example is fallow fields along woodlots, which result in false identification of *Phragmites* in a linear patch along the treeline. These errors were reduced as much as possible by clumping and sieving, but further filtering would actually remove true classes.

There is some confusion of agriculture with many of the LULC classes (Table 5). Agricultural land often borders many of these LULC types and, depending on the crop planted, it can look spectrally similar to various LULC types. In addition, many of the agricultural lands are former wetlands and therefore may exhibit hydrological changes similar to intact wetlands, thus appearing "wet" in the PALSAR data.

Due to the high confusion of *Schoenoplectus* with open water, the maps were adjusted post-classification to correct the problem. Using all available field data, a spatial query was conducted to retain areas mapped as *Schoenoplectus* that were field verified and relabel all other areas mapped as *Schoenoplectus* to open water. Unfortunately, using all field data to make the correction did not allow for an independent assessment of the new *Schoenoplectus* class accuracy. In making this adjustment some true *Schoenoplectus* areas are likely lost, but with the high errors from the unadjusted map it was justifiable.

5.2. Importance of SAR-Optical Fusion in Wetland Mapping

The plot of band importance for the St. Clair Flats AOI (Figure 8) shows that the most important bands for wetland type mapping when using three-season Landsat TM and PALSAR data were spring

Landsat TM NDVI, spring Landsat TM thermal, and spring L-HH, followed by L-HV from summer and L-HH from fall. The PALSAR L-HH band (which is sensitive to moisture/inundation), along with the spring Landsat TM NDVI and thermal band, are particularly important to the classification, and that importance was consistent across AOIs with large regions of wetland cover. However, for classifications generated in areas with a greater percentage of urban and suburban coverage (Figure 9), the output maps relied more heavily on the visible Landsat TM bands, and the PALSAR L-HV bands were ranked 12th, 13th and 14th, slightly above the L-HH bands (ranked 17–19th). L-HV is more sensitive to biomass than moisture and Landsat TM bands are most useful for distinguishing upland cover types. It is for the wetland classes that PALSAR L-HH is of such high utility, as seen in Figure 8. However, the L-HV band, with its sensitivity to structure and biomass, aids in distinguishing shrub from forest from herbaceous wetland. It is notable that the thermal channel is of high importance (ranking 1st or 2nd) for both wetland-dominated AOIs and urban/suburban-dominated AOIs. The thermal band, in conjunction with NDVI, has been shown to be effective for LULC classification [43–45]. Water has a high thermal inertia, therefore the temperature of water and wetlands changes more slowly than for surrounding uplands. In the summer, water is generally cooler than the land, and in the winter, it is warmer. Additionally, evapotranspiration from vegetation results in cooler temperatures than from barren or sparsely vegetated LULC classes [44]. Urban environments are also typically warmer due to solar heating of paved surfaces and heat generated from anthropogenic sources [45].

Other researchers have noted the importance of L-band in detection of woody wetlands (in particular [20,24,46]) and for detection of the large, dense forming invasive wetland grass *Phragmites* in the coastal Great Lakes [26]. L-band fused with optical data has been helpful in overall wetland mapping, such as for tropical peatland types in Peru [41], and when combined with C-band dual-band/dual-season data for distinguishing and mapping a diverse set of ecosystems in the vast wetland complexes of the Pantanal in South America [42]. Whereas most researchers find the L-HH band to be of greatest utility for wetland mapping due to its ability to detect inundation, others note the usefulness of the L-HV band for differentiating vegetation structure in wetlands (e.g., [41]).

For the coastal Great Lakes map presented here, both L-HH and L-HV were found to be of high importance in wetland mapping. The methods developed for mapping coastal wetlands of the Great Lakes are unique in fusing three season Landsat 5 TM, including the thermal band, and three-season PALSAR L-HH/L-HV data over a large region. Whereas others have investigated multi-sensor fusion, and some have used dual-season multi-sensor fusion, few have used three-season datasets and most remove the Landsat 5 TM thermal band. The three-season data are crucial because they capture the phenologic differences in the vegetation and the seasonal variation in the hydrology. For example, *Typha* stands are typically fallen over in the spring with high water; in summer they are at peak vegetation height and density with lower water tables and less distinguishable from other wetland types. In contrast, stands of *Phragmites* have significant standing dead biomass in the spring that remains in the summer as new shoots sprout up. Using summer data alone makes distinguishing these two genera difficult, but using the phenology of the vegetation aids in distinguishing them, and the patterns of hydroperiod distinguish the wetlands from the uplands. Some of the wetlands are wet in spring and fall, such as the forested wetlands, and that provides two chances to detect the inundation, depending on the timing of the satellite collections.

The SAR-optical technique for mapping Great Lakes wetlands was demonstrated as a repeatable, high accuracy, and timely method (3.5 years including development of mapping methodology) that can be applied to large regional areas while integrating high accuracy image interpretation, field data and moderate spatial resolution remote sensing in a sophisticated machine-learning approach. Such an approach has wide applicability beyond the coastal wetlands of the Great Lakes. This approach to wetland mapping has been applied to non-coastal temperate regions, including the state of Michigan and the state of Maine, as well as to boreal peatlands of Alberta [47] and is currently being applied to map tropical peatlands of Peru.

6. Summary and Significance

The Great Lakes bi-national coastal wetland product represents a current, circa 2010, comprehensive basin-wide inventory of coastal wetlands, as defined by USFWS NWI types with additional classes for dominant plant species *Phragmites*, *Schoenoplectus spp*. and *Typha spp* and adjacent LULC classes as defined in the GLCWC Monitoring Plan protocol [6]. This effort represents the first comprehensive wetland delineation of the bi-national coastal Great Lakes using a consistent mapping technique. The map provides information not only on wetland extent and type, but also contemporary information on potential wetland stressors (e.g., invasive plant species and level and type of development surrounding the wetlands). More specifically, the map is designed to assist in identifying indicators of wetland health defined through the State of the Lakes Ecosystem Conference, including: (1) land cover adjacent to coastal wetlands; (2) land cover/land conversion; (3) urban density; (4) non-native terrestrial species, and (5) wetland extent and composition [48]. It was also developed to provide reference and input for the GLIC, which has a five-year plan for collection of biologic and other field-based indicators of wetland health throughout the Great Lakes [6].

Although the map produced represents a static point in time depicting the distribution of wetlands by type across the basin, it serves as a baseline for future mapping of change. The mapping methodology used is reproducible, allowing for the continual development of future maps for monitoring and detecting change in the Great Lakes Basin. With the launch of Landsat 8 in 2013 and PALSAR-2 in 2014, map updates and changes can be made in the next few years. The German Aerospace Center (DLR) has plans to launch L-band satellites (Tandem-L), as do NASA, India with NISAR (L-band and S-band SAR sensors), and Argentina with SAOCOM–1, thus extending the mapping capability into the longer-term future. In addition, mapping past conditions circa 1997 is possible with JERS-1 (predecessor to PALSAR) and Landsat 5 TM. A change mapping technique, such as is conducted by NOAA for C-CAP, could be applied to the hybrid PALSAR-Landsat methodology for efficiency.

Acknowledgments

The work presented was supported by the Great Lakes Restoration Initiative through a grant from the U.S. EPA. Although the research described in the article has been funded wholly or in part by the U.S. Environmental Protection Agency's GLNPO office through grant (GL-00E00559-0), it has not been subjected to any EPA review and therefore does not necessarily reflect the views of the Agency, and no official endorsement should be inferred. We acknowledge Jane Whitcomb, Mahta Moghaddam, Kirk Scarbrough, and Richard Powell for their contributions to the early work and research.

The authors thank field interns Nicole Uebbing, Caroline Keson, Caleigh Hoiland, Rachel Posavetz, Daniel Hutchison, and Kaitlyn Smith for their assistance in the field. We thank Nor Serocki for her help with references and formatting. Lastly, we acknowledge Dante Mann for his assistance with figures and formatting.

Author Contributions

Laura Bourgeau-Chavez planned the mapping methods, oversaw the field collections and data processing and analysis, and wrote much of the manuscript. Sarah Endres, Michael Battaglia, and Zachary Laubach helped test methods, collected field data, interpreted air photos, created the classified maps, and wrote sections of the manuscript. Elizabeth Banda helped plan and organize field data collection. Mary Ellen Miller developed and implemented the final mapping protocol in Random Forests and wrote sections of the manuscript. Phyllis Higman oversaw the field data collection and protocol implementation for 2012–2013 field data collections. Pat Chow-Fraser and her student, James Marcaccio, provided access to the 2007 Georgian Bay field data and implemented the field collection protocol at sites along lakes Erie, Huron, and Ontario coastlines.

Conflicts of Interest

The authors declare no conflicts of interest.

References

1. Albert, D.A.; Wilcox, D.A.; Ingram, J.W.; Thompson, T.A. Hydrogeomorphic classification for Great Lakes coastal wetlands. *J. Great Lakes Res.* **2005**, *31*, 129–146.
2. Bates, B.C.; Kundzewicz, Z.W.; Wu, S.; Palutikof, J.P. Climate change and water. In *Technical Paper of the Intergovernmental Panel on Climate Change Edition 2008*; IPCC Secretariat: Geneva, Switzerland, 2008; p. 210.
3. Dahl, T.E. *Wetlands: Losses in the United States*, 1st ed.; U.S. Fish and Wildlife Service: St. Petersburg, FL, USA, 1990; p. 13.
4. Great Lakes Coastal Wetlands. *Monitoring Plan*, 1st ed.; Burton, T.M., Brazner, J.C., Ciborowski, J.J.H., Grabas, G.P., Hummer, J., Schneider, J., Uzarski, D.G., Eds.; Great Lakes Commission: Ann Arbor, MI, USA, 2008; pp. 1–283.
5. Ingram, J.; Holmes, K.; Grabas, G.; Watton, P.; Potter, B.; Gomer, T.; Stow, N. *Development of a Coastal Wetlands Database for the Great Lakes Canadian Shoreline*; Wetlands2-EPA-03; Final Report to the Great Lakes Commission: Ann Arbor, MI, USA, 2004; p. 18.
6. Bourgeau-Chavez, L.L.; Lopez, R.D.; Trebitz, A.; Hollenhorst, T.; Host, G.E.; Huberty, B.; Gauthier, R.L.; Hummer, J. Chapter 8: Landscape-based indicators. In *Great Lakes Coastal Wetlands Monitoring Plan*; U.S. EPA GLNPO 2008; Great Lakes Coastal Wetlands Consortium, Project of the Great Lakes Commission: Ann Arbor, MI, USA, 2008; pp. 143–171.

7. Wang, J.; Wang, X.; Hu, J.; Gao, Y. Preliminary study on land use classification based on multi-source remotely sensed data fusion technology. In Proceedings of the 2010 International Conference on Environmental. Science and Information Application Technology (ESIAT), Wuhan, China, 17–18 July 2010; Volume 2, pp. 5–9.
8. Lozano-Garcia, D.F.; Hoffer, R.M. Synergistic effects of combined Landsat-TM and SIR-B data for forest resources assessment. *Int. J. Remote Sens.* **1993**, *14*, 2677–2694.
9. Bourgeau-Chavez, L.L; Riordan, K.; Nowels, M.; Miller, N. *Final Report to the Great Lakes Commission: Remotely Monitoring Great Lakes Coastal Wetlands Using a Hybrid Radar and Multi-Spectral Sensor Approach*; Project No. WETLANDS2-WPA-06. 82; Great Lakes Commission: Ann Arbor, MI, USA, 2004.
10. Grenier, M.; Demers, A.; Labrecque, S.; Benoit, M.; Fournier, R.A.; Drolet, B. An object-based method to map wetland using RADARSAT-1 and Landsat ETM images: test case on two sites in Quebec, Canada. *Can. J. Remote Sens.* **2007**, *33*, 528–545.
11. Augustenijn, M.F.; Warrender, C.E. Wetland Classification using optical and radar data and neural network classification. *Int. J. Remote Sens.* **1998**, *19*, 1545–1560.
12. Corcoran, J.; Knight, J.; Brisco, B.; Kaya, S.; Cull, A.; Murnaghan, K. The integration of optical, topographic, and radar data for wetland mapping in northern Minnesota. *Can. J. Remote Sens.* **2012**, *37*, 564–582.
13. Fournier, R.A.; Grenier, M.; Lavoie, A.; Hélie, R. Towards a strategy to implement the Canadian Wetland Inventory using satellite remote sensing. *Can. J. Remote Sens.* **2007**, *33*, S1–S16.
14. Margono, B.A.; Potapov, P.V.; Turubanova, S.; Stolle, F.; Hansen, M.C. Primary forest cover loss in Indonesia over 2000–2012. *Nat. Clim. Chang.* **2014**, *4*, 730–735.
15. Ozesmi, S.L.; Bauer, M.E. Satellite remote sensing of wetlands. *Wetl. Ecol. Manag.* **2002**, *10*, 381–402.
16. Whitcomb, J.B.; Moghaddam, M.; McDonald, K.; Kellndorfer, J.; Podest, E. Mapping vegetated wetlands of Alaska using L-band radar satellite imagery. *Can. J. Remote Sens.* **2009**, *35*, 54–72.
17. Arzandeh, S.; Wang, J. Texture evaluation of RADARSAT imagery for wetland mapping. *Can. J. Remote. Sens.* **2002**, *28*, 653–666.
18. Rao, B.R.; Dwivedi, R.S.; Kushwaha, S.P.S.; Bhattacharya, S.N.; Anand, J.B.; Dasgupta, S. Monitoring the spatial extent of coastal wetlands using ERS-1 SAR data. *Int. J. Remote Sens.* **1999**, *20*, 2509–2517.
19. Hess, L.L.; Melack, J.M.; Simonett, D.S. Radar detection of flooding beneath the forest canopy: A review. *Int. J. Remote Sens.* **1990**, *11*, 1313–1325.
20. Hess, L.; Melack, J.; Filoso, S.; Wang, Y. Delineation of inundated area and vegetation along the Amazon floodplain with the SIR-C synthetic aperture radar. *IEEE Trans. Geosci. Remote Sens.* **1995**, *4*, 896–904.
21. Bourgeau-Chavez, L.L.; Kasischke, E.S.; Brunzell, S.M.; Mudd, J.P.; Smith, K.B.; Frick, A.L. Analysis of space-borne SAR data for wetland mapping in Virginia riparian ecosystems. *Int. J. Remote Sens.* **2001**, *22*, 3665–3687.
22. Pope, K.O.; Rey-Benayas, J.M.; Paris, J.F. Radar remote sensing of forest and wetland ecosystems in the Central American tropics. *Remote Sens. Environ.* **1994**, *48*, 205–219.

23. Touzi, R.; Deschamps, A.; Rother, G. Wetland characterization using polarimetric RADARSAT-2. *Can. J. Remote Sens.* **2007**, *33*, S56–S67.
24. Lang, M.W.; Kasischke, E.S. Using C-band synthetic aperture radar data to monitor forested wetland hydrology in Maryland's coastal plain, USA. *IEEE Trans. Geosci. Remote Sens.* **2008**, *46*, 535–546.
25. Baghdadi, N.; Bernier, M.; Gauthier, R.; Neeson, I. Evaluation of C-band SAR data for wetlands mapping. *Int. J. Remote Sens.* **2001**, *22*, 71–88.
26. Bourgeau-Chavez, L.L.; Kowalski, K.P.; Carlson Mazur, M.L.; Scarbrough, K.A.; Powell, R.B.; Brooks, C.N.; Huberty, B.; Jenkins, L.K.; Banda, E.C.; Galbraith, D.M.; *et al*. Mapping invasive Phragmites australis in the coastal Great Lakes with ALOS PALSAR satellite imagery for decision support. *J. Great Lakes Res. Suppl.* **2013**, *39*, 65–77.
27. Fujimura, S.; Kiysau, S. Clasification of terrain objects using hyper-dimensional (multi-temporal multi-spectral) images through pupose-oriented feature extraction. In Proceedings of the Geoscience and Remote Sensing Symposium, Hamburg, Germany, 28 June–2 July 1999; Volume 2, pp. 1192–1194.
28. Shang, J.; McNarin, H.; Champagne, C.; Jiao, X. Contribution of multi-frequency, multi-sensor, and multi-temporal radar data to operational annual crop mapping. In Proceedings of the IEEE International Geoscience and Remote Sensing Symposium, IGARSS 2008, Boston, MA, USA, 7–11 July 2008; Volume 3, III-378–III-381.
29. Schmidt, K.S.; Skidmore, A.K. Spectral discrimination of vegetation types in coastal wetland. *Remote Sens. Environ.* **2003**, *8*, 92–108.
30. Becker, B.L.; Lusch, D.P.; Qi, J. Identifying optimal spectral bands from *in situ* measurements of Great Lakes coastal wetlands using second-derivative analysis. *Remote Sens. Environ.* **2005**, *97*, 238–248.
31. Rebelo, L.S. Eco-hydrological characterization of inland wetlands in Africa using L-band SAR. *Sel. Top. Appl. Earth Obs. Remote Sens. IEE J.* **2010**, *3*, 554–559.
32. Masek, J.G.; Vermote, E.F.; Saleous, N.E.; Wolfe, R.; Hall, F.G.; Huemmrich, F.; Gao, F.; Kutler, J.; Lim, T.K. A Landsat surface reflectance data set for North America, 1990–2000. *IEEE Geosci. Remote Sens. Lett.* **2006**, *3*, 69–72.
33. Homer, C.; Dewitz, J.; Fry, J.; Coan, M.; Hossain, N.; Larson, C.; Herold, N.; McKerrow, A.; van Driel, J.N.; Wickham, J. Completion of the 2001 national land cover database for the conterminous United States. *Photogram. Eng. Remote Sens.* **2007**, *73*, 337–341.
34. Wulder, M.A.; Dechka, J.A.; Gillis, M.A.; Luther, J.E.; Hall, R.J.; Beaudoin, A.; Franklin, S.E. Operational mapping of the land cover of the forested area of Canada with Landsat data: EOSD land cover program. *For. Chron.* **2003**, *79*, 1–9.
35. Rouse, J.W.; Hass, R.H.; Schell, J.A.; Deering, D.W. *Monitoring Vegetation Systems in the Great Plains with ERTS*; NASA Special Publication: Washington, DC, USA, 1974.
36. Breiman, L. Random Forests. *Mach. Learn.* **2001**, *45*, 5–32.
37. Liaw, A.; Wiener, M. Classification and regression by random forest. *R. News* **2002**, *2*, 18–22.
38. Anderson, J.R.; Hardy, E.E. Roach, J.T.; Witmer, R.E. *A Land Use and Land Cover Classification System for Use with Remote Sensor Data*; U.S. Geographical Survey Circular: Washington, DC, USA, 1976.

39. Congalton, R.; Green, K. *Assessing the Accuracy of Remotely Sensed Data: Principles and Practices*, 2nd ed.; CRC/Taylor & Francis: Boca Raton, FL, USA, 2008.
40. Great Lakes Coastal Wetland Maps. Available online: http://geodjango.mtri.org/coastal-wetlands (accessed on 23 June 2015).
41. Draper, F.C.; Roucoux, K.H.; Lawson, I.T.; Mitchard, E.T.A.; Honorio Coronado, E.N.; Lähteenoja, O.; Montenegro, L.T.; Sandoval, E.V.; Zaráte, R.; Baker, T.R. The distribution and amount of carbon in the largest peatland complex in Amazonia. *Environ. Res. Lett.* **2014**, *9*, 1–12.
42. Evans, T.L.; Costa, M.; Tomas, W.M.; Camilo, A.R. Large-scale habitat mapping of the Brazilian Pantanal wetland: A synthetic aperture radar approach. *Remote Sens. Environ.* **2014**, *155*, 89–108.
43. Baker, C.; Lawrence, R.; Montagne, C.; Patten, D. Mapping wetlands and riparian areas using Landsat ETM+ imagery and decision-tree-based models. *Wetlands* **2006**, *26*, 465–474.
44. Melesse, A.M.; Graham, W.D.; Jordan, J.D. Spatially distributed watershed mapping and modeling: thermal maps and vegetation indices to enhance land cover and surface microclimate mapping (part 1). *J. Spat. Hydrol.* **2003**, *3*, 1–29.
45. Southworth, J. An assessment of Landsat TM band 6 thermal data for analysing land cover in tropical dry forest regions. *Int. J. Remote Sens.* **2004**, *25*, 689–706.
46. Townsend, P.A. Estimating forest structure in wetlands using multitemporal SAR. *Remote Sens. Environ.* **2002**, *79*, 288–304.
47. Bourgeau-Chavez, L.L.; Endres, S.; Banda, E.; Powell, R.; Turetsky, M.R.; Benscoter, B.; Kasischke, E.S. Classification of Boreal Peatland Ecosystem types with Hybrid Multi-Temporal Satellite Radar and Optical Imagery for Analysis of Vulnerability to Wildfire. *Int. J. Wildland Fire* **2015**, submitted.
48. United States Environmental Protection Agency. Available online: http://www.epa.gov/solec/ (accessed on 23 June 2015).